Energy Extraction from a Slider-Crank Wave Energy under Irregular Wave Conditions

Preprint

Y. Sang, H. Bora Karayaka, and Y. Yan
Western Carolina University

J.Z. Zhang
Kettering University

E. Muljadi and Y.H. Yu
National Renewable Energy Laboratory

To be presented at OCEANS
Washington, D.C.
October 19–22, 2015

NREL is a national laboratory of the U.S. Department of Energy
Office of Energy Efficiency & Renewable Energy
Operated by the Alliance for Sustainable Energy, LLC

This report is available at no cost from the National Renewable Energy Laboratory (NREL) at www.nrel.gov/publications.

Conference Paper
NREL/CP-5D00-64875
August 2015

Contract No. DE-AC36-08GO28308

NOTICE

This report is available at no cost from the National Renewable Energy Laboratory (NREL) at www.nrel.gov/publications.

Available electronically at SciTech Connect http:/www.osti.gov/scitech

Available for a processing fee to U.S. Department of Energy and its contractors, in paper, from:

U.S. Department of Energy
Office of Scientific and Technical Information
P.O. Box 62
Oak Ridge, TN 37831-0062
OSTI http://www.osti.gov
Phone: 865.576.8401
Fax: 865.576.5728
Email: reports@osti.gov

Available for sale to the public, in paper, from:

U.S. Department of Commerce
National Technical Information Service
5301 Shawnee Road
Alexandria, VA 22312
NTIS http://www.ntis.gov
Phone: 800.553.6847 or 703.605.6000
Fax: 703.605.6900
Email: orders@ntis.gov

Cover Photos by Dennis Schroeder: (left to right) NREL 26173, NREL 18302, NREL 19758, NREL 29642, NREL 19795.

NREL prints on paper that contains recycled content.

Energy Extraction from A Slider-Crank Wave Energy Converter under Irregular Wave Conditions

Yuanrui Sang, H. Bora Karayaka, Yanjun Yan
Department of Engineering and Technology
Western Carolina University
Cullowhee, North Carolina 28723, USA
hbkarayaka@wcu.edu

James Z. Zhang
Kettering University
1700 University Avenue
Flint, MI 48504, USA

Eduard Muljadi, Yi-Hsiang Yu
National Renewable Energy Laboratory
15013 Denver West Parkway
Golden, Colorado 80401, USA

***Abstract* — A slider-crank wave energy converter (WEC) is a novel energy conversion device. It converts wave energy into electricity at a relatively high efficiency, and it features a simple structure. Past analysis on this particular WEC has been done under regular sinusoidal wave conditions, and suboptimal energy could be achieved. This paper presents the analysis of the system under irregular wave conditions; a time-domain hydrodynamics model is adopted and a rule-based control methodology is introduced to better serve the irregular wave conditions. Results from the simulations show that the performance of the system under irregular wave conditions is different from that under regular sinusoidal wave conditions, but a reasonable amount of energy can still be extracted.**

Keywords — slider-crank; wave energy converter (WEC); ocean energy; irregular waves

I. INTRODUCTION

Ocean energy is one of the most promising renewable energy sources. The ocean covers 71% of the Earth [1], and if 0.2% of its energy could be extracted, it would produce enough power for the whole world [2]. However, at present, ocean wave energy is the most expensive type of water power because of a lack of available models of wave energy converters (WECs) [3]. This paper presents a control methodology for a novel slider-crank WEC, and its feasibility under irregular ocean wave conditions is validated through simulations.

The slider-crank power take-off system (PTOS) is a type of direct-drive rotational (DDR) PTOS. It converts ocean wave energy directly to electric power without intermediate stages involving hydraulics or pneumatics. The DDR-PTOS is a good choice for WEC deployments that are larger than 10 kW [4] because it can avoid the air-gap tolerance and linear guidance challenges that are encountered by linear generators at high power levels. Previous research has been done on DDR-PTOS such as rack-and-pinion mechanisms and traction tires/wheels [4], but research on the slider-crank PTOS is rare. Previous analysis was done on the slider-crank PTOS under regular wave conditions [5]; the suboptimal nature of the control strategy for the system was validated. However, because ideal sinusoidal wave conditions rarely exist in real oceans, it is very important to find a control methodology for the system under irregular wave conditions.

A control methodology for the slider-crank WEC under irregular wave conditions is proposed in this paper. A semi-submerged spherical buoy is applied in the system; to handle nonlinearity, a time-domain hydrodynamics model is adopted. An AC synchronous machine is used in this model because of its simplicity in modeling and control. The control methodology keeps the generator rotating in resonance with the wave excitation force so that energy can be extracted at a relatively high efficiency. The excitation force is calculated from irregular waves generated through the JONSWAP spectrum, and simulations are carried out in the MATLAB/Simulink environment. Results show that an amount of energy comparable to that from the previous research using a DDR-PTOS can be extracted [6],[7].

This paper is organized as follows. The mathematical model of the system is introduced in Section II, and the control strategy that maximizes energy extraction for irregular waves is presented in Section III. Section IV shows simulation results, and Section V discusses some considerations for test sea trials. A conclusion is provided in Section VI.

II. MODEL OF THE SYSYEM

A. Overall System Model

The system has a buoy that moves up and down with the ocean waves, and the linear motion is converted into rotation through a slider-crank structure. Then a generator can be driven. The frequency of real ocean waves is usually between 1/6 Hz and 1/10 Hz, which is between 6 rpm and 10 rpm if they move rotationally. The rated speed of the generator in this study is 1,184 rpm. If rotating at 6 rpm to 10 rpm, the generator can produce very little power. Therefore, a gearbox will be needed between the slider-crank and the generator.

B. Hydrodynamics Model

A popular semi-submerged spherical buoy is selected for analysis based on the heave hydrodynamics provided in [8]. To deal with nonlinearity, the Cummins equation [9] is introduced to describe the relationship between the buoy motion and the hydrodynamic forces, and it can be expressed as

$$(M + a_\infty)\ddot{z}(t) + \int_{-\infty}^{t} H_{rad}(t-\tau)\,\dot{z}(\tau)d\tau + S_b z(t) = F_e(t) - F_u(t) \qquad (1)$$

where z is the buoy center of the gravity displacement in heave direction, M is the physical mass of the buoy, and a_∞ is the buoy-added mass at an infinite wave period, which is half of the physical mass [10]. H_{rad} is the radiation impulse response function, as Fig. 1 shows. S_b is the hydrostatic stiffness, F_e is the wave excitation force, and F_u is the wave energy harvesting device reactionary force.

The radiation force of the buoy is approximated with analytical solutions existing for the geometry [11], then a transfer function with the input of the buoy velocity and the output of the radiation force is obtained through appropriate functions in MATLAB.

The transfer function obtained is as follows:

$$\frac{F_{rad}}{\dot{z}} = \frac{9.7\times10^4 s^3+4.4\times10^5 s^2+7.5\times10^5 s-1.6\times10^4}{s^4+4.4s^3+11.2s^2+12.3s+7.1} \quad (2)$$

where F_{rad} is the radiation force and $\dot{z}$ is the buoy velocity. It can be mathematically expressed as

$$F_{rad} = \int_{-\infty}^{t} H_{rad}(t-\tau)\,\dot{z}(\tau)d\tau \quad (3)$$

For a semi-submerged buoy, assuming small buoy displacement relative to buoy radius, the buoyancy stiffness is

$$S_b = \rho g \pi a^2 \quad (4)$$

where g is the acceleration of gravity, ρ is the density of water, and a is the radius of the buoy.

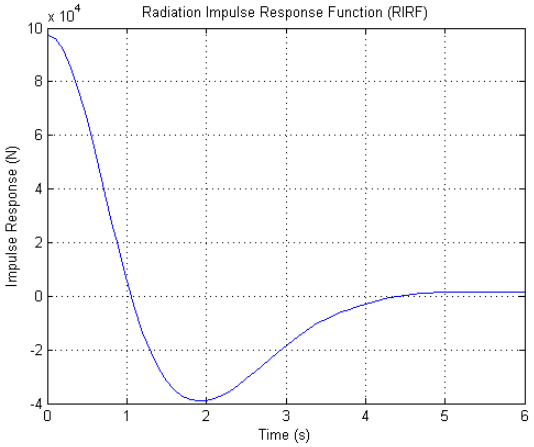

Fig. 1. Radiation impulse response function of the buoy

C. Excitation Force Calculation for Irregular Waves

An irregular wave can be composed by a number of regular sinusoidal waves with different amplitudes, angular velocities, and phases. In this research, the angular velocity is chosen in the range of 0.5 radian/s to 1.4 radian/s with an interval of 0.01 radian/s, and the interval is denoted as Δf.

The amplitudes of the irregular waves were generated with the JONSWAP spectrum, which can be expressed as [12]

$$S(f) = \frac{\alpha_j g^2}{(2\pi)^4} f^{-5} \exp\left[-\frac{5}{4}\left(\frac{f_p}{f}\right)^4\right]\gamma^{\Gamma} \quad (5)$$

where α_j is a nondimensional variable that is a function of the wind speed and fetch length, f_p is the peak frequency of the irregular wave, f is the frequency of the wave components, and γ^{Γ} is the peak enhancement factor. A value of 6 is used for γ in this study, and

$$\Gamma = \exp\left[-\left(\frac{\frac{f}{f_p}-1}{\sqrt{2}\sigma}\right)^2\right], \sigma = \begin{cases} 0.07 & f \le f_p \\ 0.09 & f > f_p \end{cases} \quad (6)$$

$$\alpha_j = \frac{H_{m0}^2}{16\int_0^{\infty} S^*(f)df} \quad (7)$$

In the above equation, H_{m0} is the significant wave height of the irregular wave, and

$$S^*(f) = \frac{g^2}{(2\pi)^4} f^{-5} \exp\left[-\frac{5}{4}\left(\frac{f_p}{f}\right)^4\right]\gamma^{\Gamma} \quad (8)$$

Significant wave heights in the simulations can be chosen according to the equal energy transport theorem [6]:

$$H_{m0} = 2\sqrt{2}A \quad (9)$$

where A is the amplitude of the regular sinusoidal wave with equal energy.

The JONSWAP spectrum is shown in Fig. 2 with a significant wave height of 1.4142 meters, which is equivalent to an amplitude of 0.5 meters for a regular wave, a peak period of 8 seconds, and γ of 6.

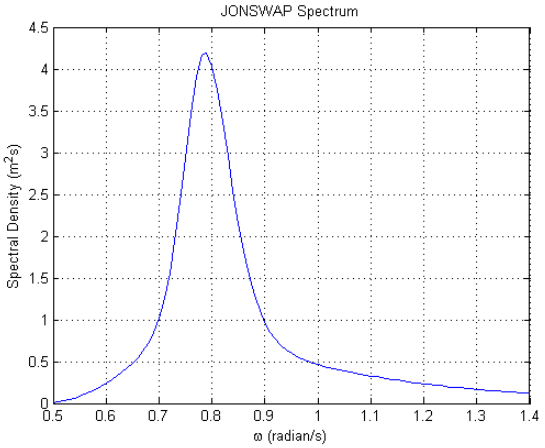

Fig. 2. An example of the JONSWAP spectrum

The amplitude of each component of the irregular wave can thus be expressed as [13]

$$A_i = \sqrt{2S(f_i)\Delta f} \quad (10)$$

The phase of each component of the irregular wave is randomly generated from 0π to 2π, and it is denoted as φ_i in this paper.

Thus, the irregular wave elevation can be expressed as the summation of all the wave components:

$$z_w = \sum_{i=1}^{N} A_i \cdot \sin(\omega_i t + \varphi_i) \quad (11)$$

where N is the total number of wave components.

The wave excitation force due to the incident wave is calculated as

$$F_e = |\kappa|\rho g \pi a^2 z_w \angle\varphi_{\kappa} \quad (12)$$

where z_w is the water surface elevation, and κ is the excitation force coefficient [14], and the amplitude, imaginary and real parts are calculated as

$$|\kappa| = \sqrt{\frac{4\varepsilon_r}{3\pi ka}} \quad (13)$$

$$Im(\kappa) = \frac{2\varepsilon_r ka}{3} \quad (14)$$

$$Re(\kappa) = \sqrt{|\kappa|^2 - [Im(\kappa)]^2} \quad (15)$$

Where the radiation resistance coefficient, ε_r, is a function of the product of k and a and will be calculated as suggested in the literature [8],[10]. For infinite water depth, wave number, k, can be calculated as

$$k = \frac{\omega^2}{g} = \frac{2\pi}{\lambda} \quad (16)$$

The phase angle of κ can be calculated as

$$\angle\varphi_\kappa = atan\left(\frac{Im(\kappa)}{Re(\kappa)}\right) \quad (17)$$

D. PTOS Model

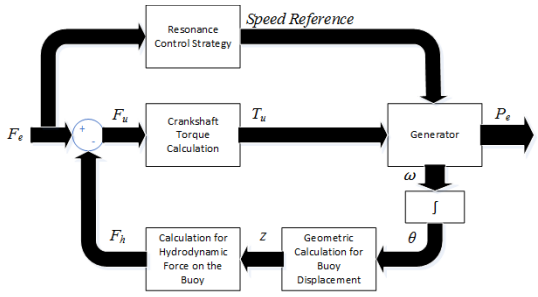

Fig. 3. Block diagram of the system

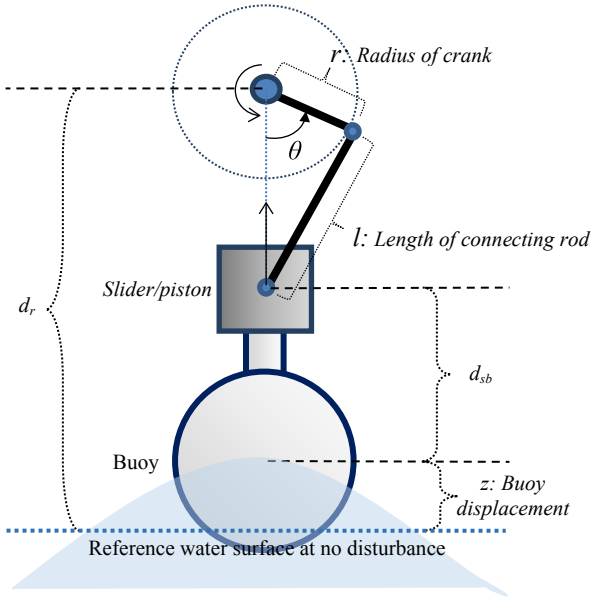

Fig. 4. Parameters of the WEC system

The generator shaft angle is obtained and fed into the hydrodynamics component (buoy), and the buoy displacement is obtained from the geometric relationship between the buoy displacement and the motion of the slider-crank:

$$z = d_r - d_{sb} - r \cdot cos\theta - \sqrt{l^2 - (r \cdot sin\theta)^2} \quad (18)$$

The system block diagram is provided in Fig. 3, where P_e is the electric power output, and a number of parameters of the WEC are illustrated in Fig. 4.

III. Control Methodology

To improve generation efficiency, a control strategy is applied on the generator to keep it rotating at a frequency that is the product of the wave frequency and the gear ratio so that the generator rotates in resonance with the wave excitation force.

A. The Rule-Based Angle Control Algorithm

The control algorithm detects the zero crossings of the wave excitation force and records the real time. Whenever a zero crossing is detected, a newly predicted half period for the next half period of wave is adopted. Then an angle reference is generated through linear extrapolation:

$$\theta_{ref} = \theta_{old} + \pi\frac{t}{T} \quad (1)$$

where θ_{old} is the angle of the electric machine at the end of last half period, T is the predicted half period of the wave, and t is the time elapsed after the zero crossing.

In the meantime, the shaft angle of the generator is detected and compared to the reference. Then a rule-based angle control algorithm determines the reference speed for the motor drive system. The rule can be summarized as follows:

$$\omega_{ref} = \frac{\pi g_r}{T}\left[1 + \left(\theta_{ref} - \theta\right)\delta\right] \quad (4)$$

$$\omega_{ref} = \begin{cases} \omega_{max}, & \text{if } \omega_{ref} > \omega_{max} \\ \omega_{min}, & \text{if } \omega_{ref} < \omega_{min} \end{cases} \quad (5)$$

where ω_{ref} is the reference speed, g_r is the gear ratio between the slider-crank and the electric machine, $\frac{\pi g_r}{T}$ is the average angular velocity of the electric machine throughout the predicted future half period of the wave, θ is the actual angle of the electric machine, δ is the increment constant, and ω_{max} and ω_{min} are the maximum and minimum of the reference speed, respectively. The reference speed later passes through a first-order IIR low-pass filter with a time constant of 0.5 second to improve noise immunity and disturbance rejection capability.

In this manner, continuous rotation of the generator at relatively high efficiency can be achieved. The proposed angle controller is illustrated with a flowchart in Fig. 5.

B. The Half-Period Prediction

To maintain the resonance between the slider-crank and the generator, a prediction of wave excitation force would be necessary. As explained in the previous section, in the proposed control methodology a prediction of only the half-force period ahead is needed, not the full prediction of the force amplitude within that half period. This feature of the proposed control methodology greatly alleviates the challenge in predicting wave excitation force.

A method to conveniently predict future waves is using past-wave data, and there are several models for this method. According to [15], the autoregressive (AR) model is a relatively simple and accurate method for low-frequency wave prediction. In [15], wave elevation was predicted. In this study, excitation force is predicted. Excitation force nearly follows wave elevation, and the AR model is found to be effective in

excitation force prediction, too. The AR model with an order of 10 is adopted for the half-period prediction in this study. A prediction horizon of 5 seconds is utilized to account for the maximum half period that can be encountered. An example of the predicted wave excitation force using the first three cycles of wave excitation force as training data is shown in Fig. 6. In this figure, the red curve is the predicted data, and the blue dotted curve is the original data. This figure shows that the period of the predicted wave excitation force is very close to the original one. There are some errors in amplitude at the peaks and valleys of the curve, but the amplitudes of future waves are not needed, as mentioned before.

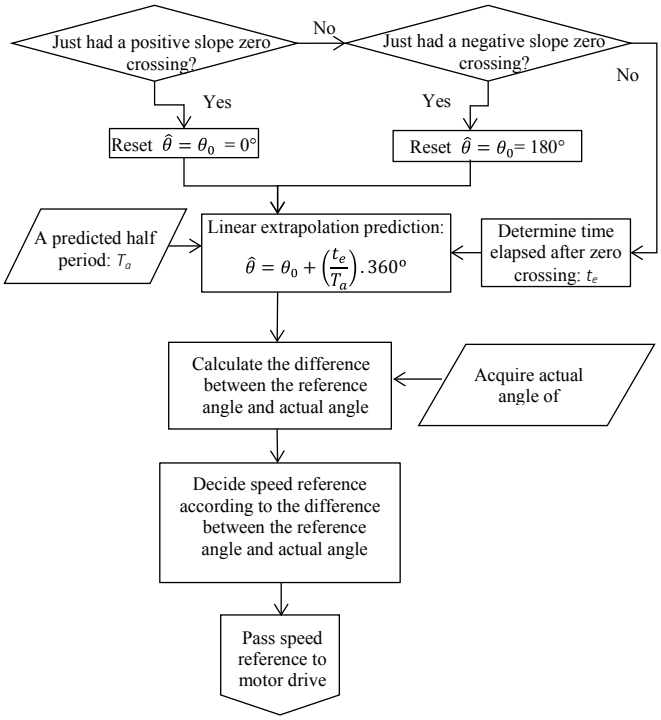

Fig. 5. Flowchart of the control algorithm

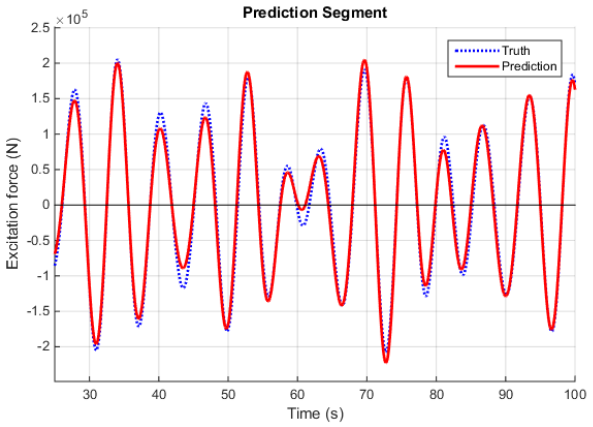

Fig. 6. Prediction of wave excitation force using the AR model

In this study, because the predicted future half periods are fairly accurate, as explained above, exact values are utilized during the simulations for the sake of simplicity.

IV. Simulation Results and Discussion

A. Simulation Setup

The simulation is carried out in the MATLAB/Simulink environment. Wave excitation force array is calculated off-line according to Section II.C and imported into the Simulink model. The hydrodynamics model is established as mentioned in Section II.B, and the PTOS model is established according to Section II.D. The control schematics of the system are shown in Fig. 7.

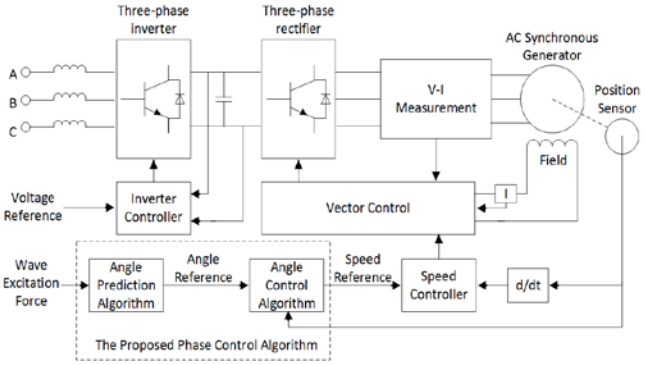

Fig. 7. Control schematics of the machine drive system

Simulations are implemented in the following steps. First, a simulation example with commonly used parameters is given in Section IV.B. Energy extraction results and system operation waveforms are provided to present its feasibility. Second, system simulations are carried out with irregular waves with different significant wave heights and peak periods to validate that the system is suitable for waves with a wide range of amplitudes and periods. A discussion about the energy extraction results is provided at the end of this section.

In the simulations of this study, parameters in Table 1 are adopted. However, the significant wave heights and peak periods associated with the irregular waves varying in different cases of simulations will be specified for each case.

Table 1. Mechanical and Generator Parameters Used in Simulations

Parameter	Value	Parameter	Value
r	0.5 m	Nominal power	149.2kW
l	1.0 m	Nominal voltage	460V
$d_r - d_{sb}$	1.0 m	Viscous friction coefficient	0.005N/(m/s)
ρ	1020 kg/m^2	Stator resistance	$2.01\times10^{-3}\Omega$
g	9.81 N/kg	Stator leakage inductance	4.289×10^{-4}H
R_v	10 kg/s	Field resistance	$4.083\times10^{-4}\Omega$
R_f	0	Field leakage inductance	0.429×10^{-3}H
$m_{cr} - m_p$	10 kg	D-axis resistance	$8.25\times10^{-3}\Omega$
buoy radius (a)	5 m	D-axis leakage inductance	0.685×10^{-3}H
PTOS gear ratio	110	Q-axis resistance	$13.89\times10^{-3}\Omega$
Generator's moment of inertia	15 kg·m^2	Q-axis leakage Inductance	1.44×10^{-3}H
Number of poles	6	D-axis mutual inductance	4.477×10^{-3}H
--	--	Q-axis mutual inductance	1.354×10^{-3}H

B. A Simulation Example

To show the details of the system's performance, a simulation example is provided first. In this simulation example, the significant wave height of the irregular wave was 1.4142 meters, and the peak period was 8 seconds. The irregular wave profile is shown in Fig. 8. The simulation was run for 250 seconds. In this case, the average electric power production was 33.0276 kW, and the cumulative energy production during the 250-second period is shown in Fig. 9.

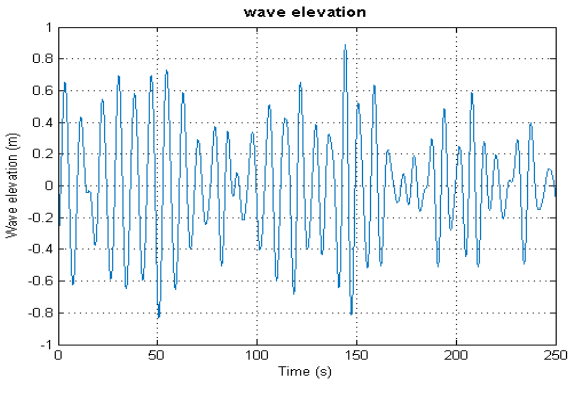

Fig. 8. Wave elevation

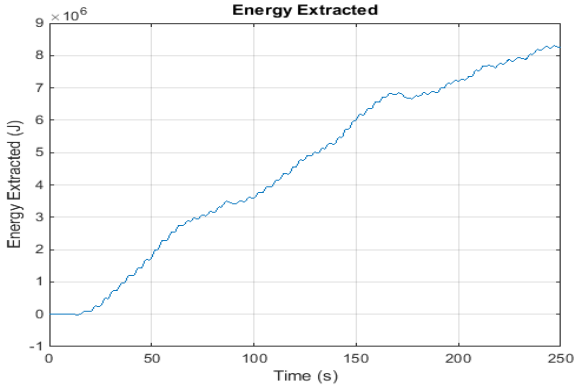

Fig. 9. Cumulative electric energy production

To reveal details about the system operation, detailed operation data from the 100th second to the 200th second are shown in the following figures. The generator shaft speed is shown in Fig. 10. The blue curve is the shaft speed reference, and the red curve is the actual generator shaft speed in the simulation. The figure shows that the control algorithm effectively maintained the generator speed consistent with its reference. Fig. 11 shows the shaft angle of the generator, Fig. 12 shows the buoy velocity, and Fig. 13 shows the wave excitation force. From the three plots it can be observed that the shaft angle of the generator and the buoy velocity are kept in resonance with the excitation force. The PTO force is shown in Fig. 14. The DC bus voltage is shown in Fig. 15, and the voltage is maintained quite stable and the fluctuation is moderate. The electromagnetic torque of the generator is shown in Fig. 16. Positive torque means the machine is working in generator mode, whereas negative torque means it is working in motor mode. The plot shows that the machine works in generator mode most of the time, but it needs to work in motor mode at times to maintain the electric machine rotating in resonance with the wave excitation force.

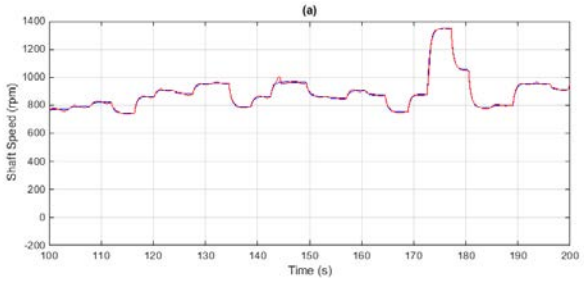

Fig. 10. Shaft speed of the AC machine

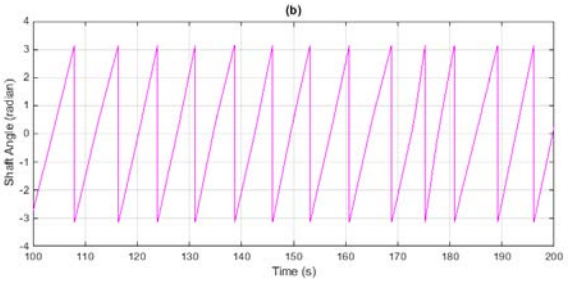

Fig. 11. Shaft angle of the AC machine

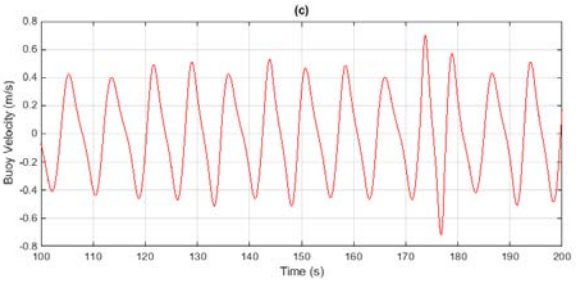

Fig. 12. Buoy velocity

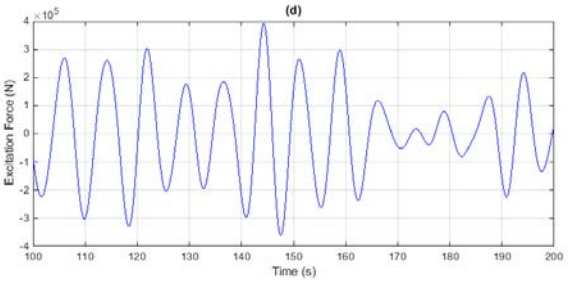

Fig. 13. Wave excitation force

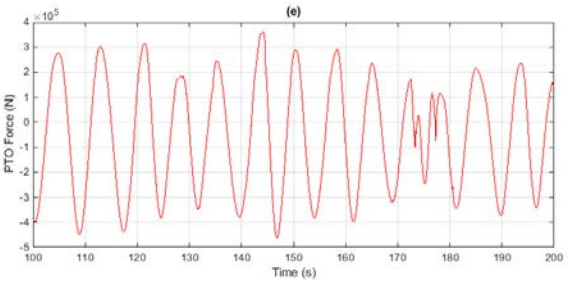

Fig. 14. PTO force

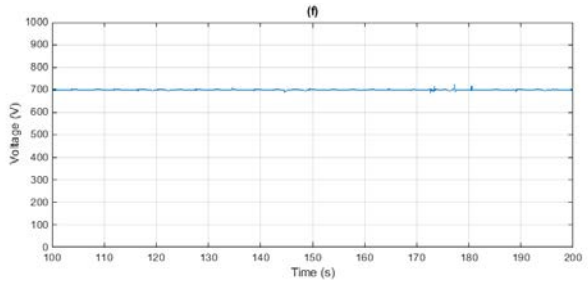

Fig. 15. DC bus voltage

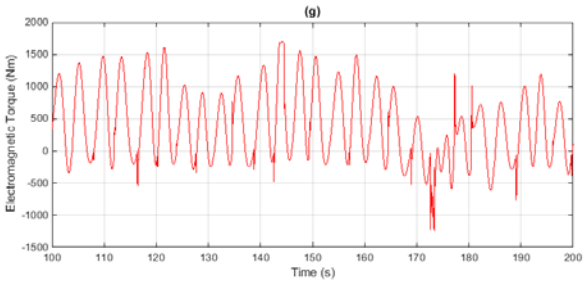

Fig. 16. Electromagnetic torque of the generator

C. *Energy Extraction with Different Significant Wave Heights and Peak Periods*

To validate the system under different wave conditions and study the influence of significant wave height and peak period on energy extraction, simulations of the system are carried out with irregular waves of four significant wave heights and five peak periods.

The significant wave heights in the simulations are chosen according to the equal energy transport theorem mentioned in Section II.C, and the significant heights of 1.1314, 1.4142, 1.6971, and 1.9799 meters are equivalent to regular wave amplitudes of 0.4, 0.5, 0.6, 0.7 meters, respectively.

All of these waves are generated with the JONSWAP spectrum and random number generator; each case is different from the other. To obtain a more accurate result, eight cases of simulations are done for each significant wave height and peak period, then an average value is calculated. The average values are provided in Table 2. Results from the 160 simulation cases validate that the system is able to work under a variety of irregular wave conditions and produce reasonable amounts of energy compared to the previous research with similar PTO conditions [6],[7].

Table 2. Average Electric Power Production at Different Significant Wave Heights and Peak Periods (kW)

T_p(s) / H_{m0}(m)	6	7	8	9	10
1.1314	16.45	22.68	26.72	28.50	26.81
1.4142	25.41	33.94	37.23	37.29	35.44
1.6971	30.69	38.22	44.76	42.74	40.58
1.9799	42.09	50.14	52.13	45.68	42.98

From the data shown in Table 2, it can be observed that the energy extraction in accordance with significant wave height and peak period shows a trend similar to that under regular wave conditions as listed in [5].

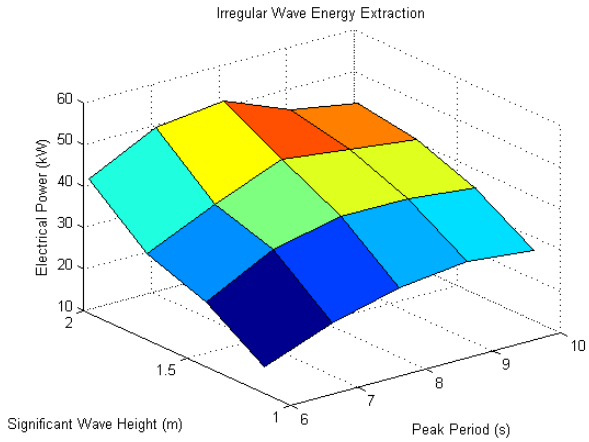

Fig. 17. Electric power production

A three-dimensional plot of the data is given in Fig. 17 to provide an intuitive illustration of the data in Table 2. Because of the torque limit of the generator, power output drops drastically at large, significant wave heights when the peak period is 9 seconds or 10 seconds, but this can be solved by selecting a generator that has a larger torque limit according to the significant wave height and peak period of the wave profile. Results from the 160 simulation cases validate that the system is able to work under irregular wave conditions and produce good amounts of energy compared to another DDR-PTOS design under similar wave conditions to [6].

V. Considerations for Test Sea Trials

This slider-crank WEC device was originally designed for deployment in offshore platforms. Parameters of the system—such as buoy size, crank radius, length of the connecting rod, and electric machine parameters—should be chosen according to the wave conditions of the location of the device so that the device can be made to best suit the local conditions. Considering the influence of currents, the height of the platform should be adjusted according to the level of the sea surface at different times of the day to maximize energy extraction, although it is possible that the system could work without adjusting its height. Coating and other protective measures should be taken into account, and regular maintenance should be conducted to reduce damage to the system caused by bio-fouling, corrosion, and water ingress. However, the detailed design of this device from the perspectives of mechanical and civil engineering is beyond the scope of this paper.

VI. Conclusion

A rule-based control methodology for a slider-crank WEC PTOS that enables it to work under irregular wave conditions is presented in this paper. Knowledge of the half-wave period is needed to ensure that the generator rotates in resonance with the wave excitation force; thus, a relatively high efficiency of energy extraction can be achieved. The control strategy requires only this future half-period duration, not the future amplitude, which greatly alleviates the prediction challenge. Time-domain hydrodynamic analysis of the buoy is adopted,

and wave excitation forces are calculated for the irregular waves generated with the JONSWAP spectrum. A study is also carried out to predict the wave excitation force by the AR model, which renders fairly accurate results. Simulations are carried out in MATLAB/Simulink, and the results show that a reasonable amount of energy can be harnessed under irregular wave conditions with different significant wave heights and peak periods compared to previous research work, validating the feasibility of the system under practical ocean wave conditions. Last, a few considerations for test sea trials are presented.

Future work of this study includes an analysis of the system with modified slider-crank parameters, incorporating excitation force predictors in real time, as well as a detailed analysis on test sea trials of this device.

VII. ACKNOWLEDGMENT

This work was supported by the Western Carolina University, Cullowhee, North Carolina and by the U.S. Department of Energy under Contract No. DE-AC36-08-GO28308 with the National Renewable Energy Laboratory.

REFERENCES

[1] National Oceanic And Atmospheric Administration. Ocean. 2014. [Online]. Available: http://www.noaa.gov/ocean.html

[2] T. Brekken, "Fundamentals of ocean wave energy conversion, modeling, and control," in Proc. 2010 IEEE International Symposium on Industrial Electronics (ISIE), Bari, Italy, pp. 3921–3966.

[3] V. S. Neary et al., "Methodology for design and economic analysis of Marine Energy Conversion (MEC) technologies," Sandia National Laboratories, Albuquerque, NM, Rep. SAND-2014-9040, 2014.

[4] K. Rhinefrank et al.. "Comparison of direct-drive power takeoff systems for ocean wave energy applications," IEEE J. Ocean. Eng., vol. 37, no.1, pp. 35–44, Jan. 2012.

[5] Y. Sang et al., "Resonance control strategy for a slider crank WEC power take-off system," in Proc. MTS/IEEE OCEANS '14, St. John's, Canada, 2014, pp. 1–8.

[6] E. Tedeschi et al., "Effect of control strategies and power take-off efficiency on the power capture from sea waves," IEEE Trans. Energy Convers., vol. 26, no. 4, pp. 1088–1098, Dec. 2011.

[7] E. Tedeschi and M. Molinas, "Tunable control strategy for wave energy converters with limited power takeoff rating," IEEE Trans. Ind. Electron., vol. 59, no. 10, pp. 3838–3846, Oct. 2012.

[8] J. Falnes, Ocean Waves and Oscillating Systems. Cambridge, MA: Cambridge University Press, 2002.

[9] W. E. Cummins, "The impulse response function and ship motions," Schiffstechnik, vol. 9, pp. 101–109, 1962.

[10] A. Hulme, "The wave forces acting on a floating hemisphere undergoing forced periodic oscillations," J. Fluid Mech., vol. 121, pp. 443–463, 1982.

[11] J. Hals, J. Falnes, and T. Moan, "Constrained optimal control of a heaving buoy wave-energy converter[J]," J. of Offshore Mechanics and Arctic Engineering, vol. 133, no. 1, 011401, Feb. 2011.

[12] K. Hasselman et al., "Measurements of wind-wave growth and swell decay during the Joint North Sea Wave Project (JONSWAP)," German Hydrographic Institute, Germany, Tech. Rep. 12, 1973.

[13] H. Yavuz, "On control of a pitching and surging wave energy converter," International Journal of Green Energy, vol. 8, no. 5, pp. 555–584, Aug. 2011.

[14] A. Kyllingstad, "Approximate analysis concerning wave-power absorption by hydrodynamically interacting buoys," Ph.D. Thesis, the Norwegian Institute of Technology, University of Trondheim, Trondheim, Norway, 1982.

[15] F. Fusco, and J. V. Ringwood, "Short-term wave forecasting for real-time control of wave energy converters," IEEE Trans. Sustainable Energy, vol. 1, no. 2, pp. 99, 106, July 2010.